

# Mode division multiplexing in a polymer-loaded plasmonic planar waveguide

Q. Q. Cheng, T. Li,\* L. Li, S. M. Wang, and S. N. Zhu

National Laboratory of Solid State Microstructures, College of Engineering and Applied Sciences, School of Physics, Nanjing University, Nanjing 210093, China

\*Corresponding author: taoli@nju.edu.cn

Received March 31, 2014; revised May 25, 2014; accepted May 27, 2014;  
posted May 28, 2014 (Doc. ID 209266); published June 25, 2014

A mode division multiplexer (MDM) based on in-plane diffractions is experimentally demonstrated in a polymer-loaded plasmonic planar waveguide. Three guided modes ( $TM_1$ ,  $TE_1$ , and  $TM_2$ ) were well demultiplexed by a focusing design with a focal length of about 40  $\mu\text{m}$ , which are clearly distinguished by the polarization control. The experimental results well reproduced the theoretical design and calculation. Moreover, the demultiplexed focal spots directly reflect the different modes, by which a mode diagram of the dielectric-loaded planar waveguide was vividly mapped out by varying the polymer layer thickness. In this regard, the proposed device may not only serve as a MDM for the integrated optics but can also provide a new strategy in analyzing the guided modes. © 2014 Optical Society of America

OCIS codes: (050.1970) Diffractive optics; (130.2790) Guided waves; (240.3990) Micro-optical devices.  
<http://dx.doi.org/10.1364/OL.39.003900>

Surface plasmon polariton (SPP) is one of the promising carriers to achieve photonic integration beyond the diffraction limit of light, although it always suffers from a huge dissipation loss of metal [1]. In recent years, the alliance of dielectric and metal in particularly designed waveguides has demonstrated much better performance in field confinement and low propagating loss in wave guiding [2–7]. In fact, introducing a dielectric layer on a metallic surface would endow the waveguide with higher ordered modes as the layer is thick enough and would possibly allow for further signal processing. Among the current kinds of key techniques, multiplexing is an important method for signal processing in information technology. In optical communications, mode division multiplexing (MDM) is regarded as a good solution to enhance optical network's capacity to avert network gridlock (e.g., in fiber-optical communication [8]). From a viewpoint of photonic on-chip integration, it is highly expected to realize the MDM in a plasmonic system. Since there are a number of guided modes accommodated in the polymer-loaded waveguide [2,5,9,10], it is reasonable to achieve the demultiplexing via well-designed nanostructures.

Recently, an in-plane diffraction method was developed to manipulate SPP beams [11–13], as well as to achieve broadband focusing and WDM [14]. Compared with the SPP on a metal surface, a polymer-loaded plasmonic waveguide supports a series of guided modes in the same frequency with different propagation wave numbers (i.e., wavelengths). In this Letter, the in-plane diffraction method is extended to a dielectric/metal waveguide system for the first time, to the best of our knowledge. With a well-designed nanohole array in the metal layer, the MDM for different guided modes (both TM and TE) is presented, which was realized by focusing multimodes to different focal spots so as to achieve the demultiplexer. Since all the guided modes can be spatially imaged, this MDM is also able to work as a mode spectrometer. Based on this, a calculated MDM mode map with respect to different polymer thickness is presented in good agreement with the theoretical mode diagram.

Before getting into the experimental details, we first review the mode properties in a polymer-loaded plasmonic [insulator/insulator/metal ( $I/I/M$ )] waveguide. According to the mode diagram of  $I/I/M$  waveguides, as shown in our previous paper [9] (also see the theoretical mode curve in Fig. 4), it is evident that with increasing the polymer thickness, more guided modes are accommodated. To be noted, the thickness of the metal has little influence on the mode property as long as it is much larger than the skin depth ( $\sim 20$   $\mu\text{m}$  for silver in the optical region). It is quite possible to introduce the diffraction process [11] to manipulate the guided modes in this  $I/I/M$  planar waveguide. Here, we will mainly analyze the modes of  $TM_1$ ,  $TE_1$ , and  $TM_2$  in the polymer-loaded waveguide with the polymer layer thickness of 560 nm, whose effective mode indices are 1.51, 1.35, and 1.14, respectively. To achieve a focusing of the guided mode, parabolic lateral phase modulation is required. According to the constructive interference at every local lattice, the diffracted guide wave (in the  $x$  direction) would have an extra  $2\pi$  phase change between neighbor lattices in its transverse direction ( $z$  axis). Therefore, the phase evolution in the  $z$  direction with respect to all diffracted guided modes can be written as

$$\varphi_m(z) = \varphi_0 + k_{\text{WG}}z - 2m\pi, \quad (1)$$

where  $\varphi_0$  and  $k_{\text{WG}}$  are the initial phase and in-plane wave vector of the guided mode, respectively, and  $m$  is the sequence number of the local lattice. When the lateral phase of the diffracted beam satisfies the one required by focusing as

$$\psi(z) = -k_{\text{WG}}z^2/2f, \quad (2)$$

where  $f$  is the focal length for a concerned guided mode, we will retrieve the position of every local lattice [14].

Figure 1 schematically shows the design of the polymer-loaded planar waveguide together with diffraction nano-array, in-coupling grating, and out-coupling slits. Here, the polymer is a kind of photo resist

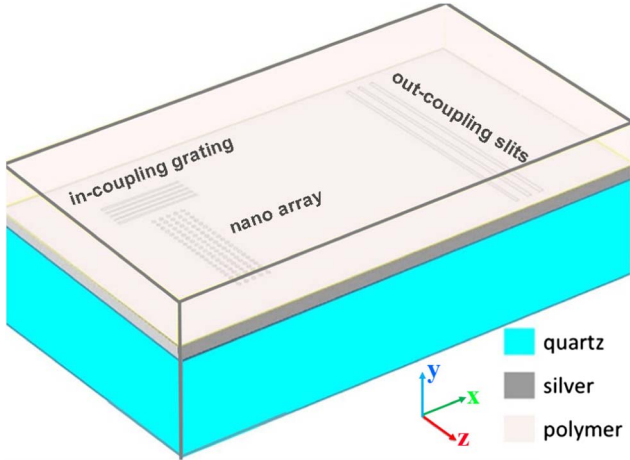


Fig. 1. Schematic of the MDM in a polymer-loaded plasmonic planar waveguide, where the horizontal grating is used for mode coupling from external incidence, the nanohole array drilled in the metal layer is for focusing the guided modes, and the slits on the right are out-coupler.

(AR-P3110, refractive index of  $n = 1.653$ ), which does not react under the illumination of the used laser of  $\lambda_0 = 633$  nm. The guided modes are launched from a focused laser by a coupling grating and then propagate into a nonperiodic nano-array. By appropriately arranging the nanoholes, the guided modes are ready to be focused on both sides. Here, we take the  $TM_2$  mode as an example, with  $k_{WG} = 1.14k_0$ . Setting a focal length of  $f = 40$   $\mu\text{m}$ , we can obtain the lattice parameter ( $a_z$ ) by solving the equation of  $\varphi_m(z) = \psi(z)$  according to Eqs. (1) and (2). The designed parameters of the graded local lattice parameter  $a_z$  in the  $z$  direction are shown in Fig. 2(a), and lattice period in the  $x$  direction is 500 nm. All nanoholes are circular with a diameter of 240 nm and depth of about 20 nm. According to the local lattice parameter, we calculated the phase data of  $TM_1$ ,  $TE_1$ , and  $TM_2$  distributed along the  $z$  axis, as the symbols show in Fig. 2(b), where the solid parabolic curves are fitted to the designed data retrieved from in-plane diffractions, showing very good coincidences. It should be noted that although the local lattice parameter is designed for the  $TM_2$  mode, the phase modulation results of other two modes ( $TE_1$  and  $TM_1$ ) also satisfy the parabolic curve quite well due to the broadband property [14]. We performed calculations based on the Huygens–Fresnel integration to simulate the diffraction processes with respect to these three guided modes, as the results show in Fig. 3(a), where focused beams are manifested as well as previous SPPs [14–17].

In experiments, the nanoholes, grating, and slits were fabricated by the focused ion beam (Strata FIB201, FEI Company) on a 100 nm thick silver film that was sputtered on a quartz substrate. Afterward, the whole device was spin-coated by a polymer layer, whose thickness (560 nm here) could be adjusted by the concentration of photo resist and the spin rate. A He–Ne laser ( $\lambda_0 = 633$  nm) was focused to the in-coupling grating (with a grating constant about 500 nm), and the optical analyses on the polymer-loaded hybrid waveguide were carried out utilizing an optical microscope with an oil-immersion objective (160 $\times$ , NA = 1.32). To detect and

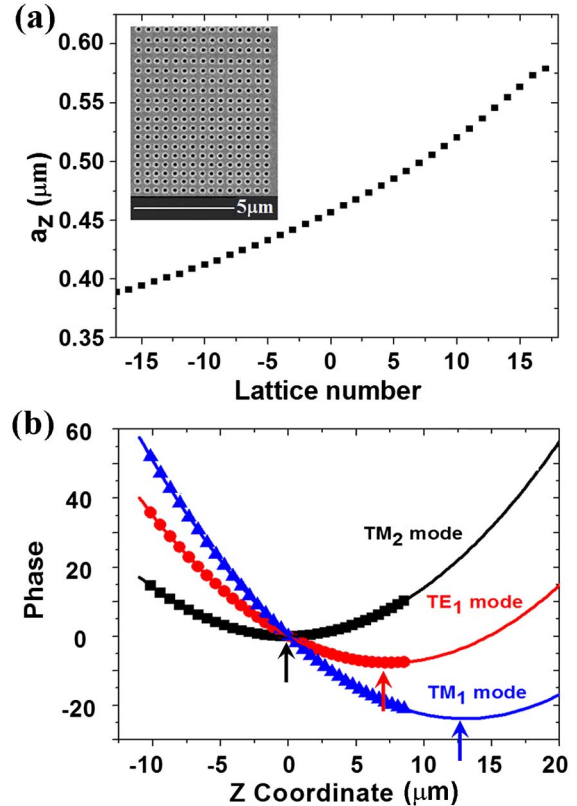


Fig. 2. (a) Lattice parameter ( $a_z$ ) of the nonperiodic array, where the inset is the SEM image of the hole array sample before being covered by the polymer. (b) Calculated phase distribution (symbols) of the guided modes with respect to the fitted parabolic curves, where the arrows indicate the symmetry centers.

analyze the focusing properties of the concerned guided modes, three slits were fabricated on the right side of the nano-array for coupling out the guided waves.

Figure 3(b) shows the experimental result, where three bright spots are well observed at the out-coupling slits,

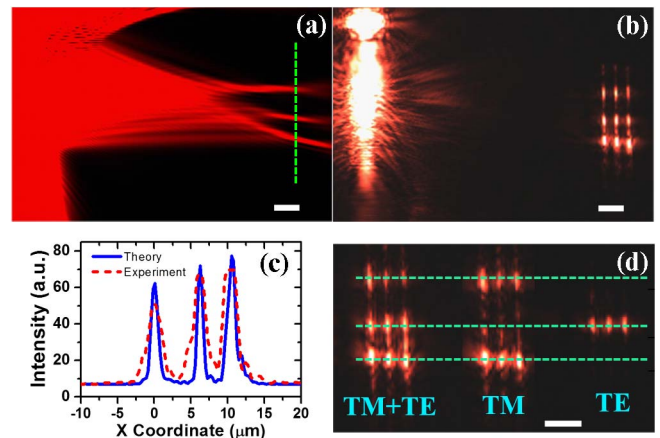


Fig. 3. (a) Calculated field distribution of three guided modes by Huygens–Fresnel integration, in which a vertical dashed line indicates the focusing distance as designed. (b) Experimental result of the focusing and demultiplexing process that was recorded by the microscopy objective. (c) Comparison of the experimental and theoretical calculations for the focused modes. (d) Polarization-tuned focusing results with good distinguished TE and TM modes (scale bar = 5  $\mu\text{m}$ ).

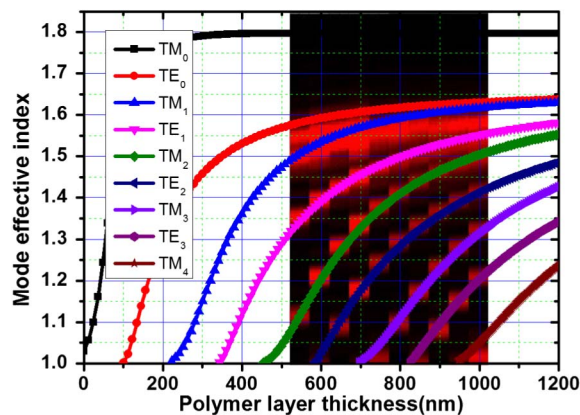


Fig. 4. Mode map retrieved from the calculated field distributions on the focal line for various polymer thicknesses, which are compared with the analytically calculated mode curves from  $TM_0$  to  $TM_4$ .

indicating three focusing processes of the guided modes. According to the mode analyses, the  $TM_1$ ,  $TE_1$ , and  $TM_2$  modes have effective mode wavelengths of 420, 470, and 550 nm, respectively. Thanks to the broadband property of this nonperiodic nano-array, these modes are all focused, which well reproduces the theoretical calculation. For a more careful investigation, we extracted the focusing data from the experiment (field distribution along the middle slit) as a comparison with the calculation result [vertical line indicated in Fig. 3(a)], as depicted in Fig. 3(c), which shows extremely good agreement. According to the theoretical design, the focal spots should be located at the positions of  $z = 0, 7.0, 12.7 \mu\text{m}$  for  $TM_2, TE_1, TM_1$  modes, respectively, corresponding to the symmetry axes of the parabolic phase curves, indicated by arrows in Fig. 2(b). Our numerical and experimental results of these focal spots in the  $z$ -dimension are about  $z = 0, 6.3, 10.7 \mu\text{m}$ , respectively, which only slightly deviate from the design. Therefore, a good MDM has been achieved in such a metal/polymer waveguide. To further demonstrate the advantage in distinguishing different modes in the polarization category, we alternate the polarization of incident laser as it couples into guide modes. Considering the scheme in Fig. 1, a V-polarized (vertical, E field along the  $z$  axis) incidence on the coupling grating corresponds to TM guided modes. In this case, only top and bottom spots are lightened [see the middle case in Fig. 3(d)]. As for the TE mode with a H-polarized (horizontal) incidence, only the middle spot is bright, as shown in the right case in Fig. 3(d). In this regard, this MDM also acts a polarization analyzer.

Furthermore, this dielectric-loaded plasmonic device works not only as a MDM but also a mode spectrometer. By changing the effective mode index, which is related to the polymer thickness in this  $I/I/M$  system, we can calculate the focusing location of every mode just like Fig. 3(a) shows. Extracting the calculated field intensity

along the focusing line for all polymer thickness cases, a mode diagram is produced, as shown in Fig. 4 (intensity map), with comparison to the analytical mode curves. Here, we only present a partially calculated mode map by the focusing process that agrees well with the theoretical one, showing this diffraction process holds the capability in mode analyses in such a planar hybrid waveguide system.

In summary, we demonstrated a demultiplexing of waveguide modes within a polymer-loaded plasmonic planar waveguide, which is fulfilled by the in-plane focusing processes with a well-designed nano-array. Besides distinguishing the guided modes including TM and TE as a MDM, the in-plane diffraction process for the focusing design also acts as a mode spectrometer that is able to manifest a mode map with respect to various polymer thicknesses. It really provides people a new strategy in manipulating and analyzing the guided modes in dielectric-metal hybrid waveguide systems.

This work is supported by the National Key Projects for Basic Researches of China (No. 2012CB921501), the National Natural Science Foundation of China (Nos. 11174136, 11322439, 11321063, 91321312), the Dengfeng Project B of Nanjing University, and PAPD of Jiangsu Higher Education Institutions.

## References

1. J. A. Schuller, E. S. Barnard, W. H. Cai, Y. C. Jun, J. S. White, and M. L. Brongersma, *Nat. Mater.* **9**, 193 (2010).
2. T. Holmgaard and S. I. Bozhevolnyi, *Phys. Rev. B* **77**, 115403 (2008).
3. D. G. Zhang, X.-C. Yuan, A. Bouhelier, P. Wang, and H. Ming, *Opt. Lett.* **35**, 408 (2010).
4. Z. Chen, T. Holmgaard, S. I. Bozhevolnyi, A. V. Krasavin, A. V. Zayats, L. Markey, and A. Dereux, *Opt. Lett.* **34**, 310 (2009).
5. D. G. Zhang, Q. Fu, X. X. Wang, Y. K. Chen, P. Wang, and H. Ming, *J. Opt.* **14**, 015003 (2012).
6. R. F. Oulton, V. J. Sorger, D. A. Genov, D. F. P. Pile, and X. Zhang, *Nat. Photonics* **2**, 496 (2008).
7. F. F. Lu, T. Li, X. P. Hu, Q. Q. Cheng, S. N. Zhu, and Y. Y. Zhu, *Opt. Lett.* **36**, 3371 (2011).
8. J. Lowery and J. Armstrong, *Opt. Express* **13**, 10003 (2005).
9. Q. Q. Cheng, T. Li, R. Y. Guo, L. Li, S. M. Wang, and S. N. Zhu, *Appl. Phys. Lett.* **101**, 171116 (2012).
10. H. Ma, A. K.-Y. Jen, and L. R. Dalton, *Adv. Mater.* **14**, 1339 (2002).
11. L. Li, T. Li, S. M. Wang, C. Zhang, and S. N. Zhu, *Phys. Rev. Lett.* **107**, 126804 (2011).
12. L. Li, T. Li, S. M. Wang, and S. N. Zhu, *Opt. Lett.* **37**, 5091 (2012).
13. L. Li, T. Li, S. M. Wang, and S. N. Zhu, *Phys. Rev. Lett.* **110**, 046807 (2013).
14. L. Li, T. Li, S. M. Wang, S. N. Zhu, and X. Zhang, *Nano Lett.* **11**, 4357 (2011).
15. C. L. Zhao and J. S. Zhang, *ACS Nano* **4**, 6433 (2010).
16. Z. W. Liu, J. M. Steele, W. Srituravanich, Y. Pikus, C. Sun, and X. Zhang, *Nano Lett.* **5**, 1726 (2005).
17. C. L. Zhao and J. S. Zhang, *Opt. Lett.* **34**, 2417 (2009).